Available online at www.eccomasproceedia.org
Eccomas Proceedia COMPDYN (2023) 2286-2295

ECCOMAS
Proceedia

COMPDYN 2023
9th ECCOMAS Thematic Conference on
Computational Methods in Structural Dynamics and Earthquake Engineering
M. Papadrakakis, M. Fragiadakis (eds.)
Athens, Greece, 12-14 June 2023

EFFECT OF CYCLIC LOAD ON THE TENSILE BEHAVIOR OF A PBO FRCM COMPOSITE

Angelo S. Calabrese, Alessandro Cagnoni, Veronica Bertolli, Tommaso D'Antino, Pierluigi Colombi, Carlo Poggi

Politecnico di Milano, Milan, Italy
e-mail: angelosavio.calabrese@polimi.it
e-mail: alessandro.cagnoni@polimi.it
e-mail: veronica.bertolli@polimi.it
e-mail: tommaso.dantino@polimi.it
e-mail: pierluigi.colombi@polimi.it
e-mail: carlo.poggi@polimi.it

Abstract

The use of externally bonded fiber-reinforced cementitious matrix (FRCM) composites represents a valid alternative to traditional techniques for the strengthening and retrofitting of existing reinforced concrete and masonry structures. FRCM composites are comprised of high strength textiles embedded within inorganic matrices and can be directly applied to the external surface of the existing structural element to increase its displacement and load capacity (i.e., axial, flexural, and shear strength). Thus, FRCM have a low invasiveness and a high strength-to-weight ratio. Recently, investigations on the bond behavior of FRCM composites showed that the presence of friction between the textile and matrix can induce damage to the fiber, which in turn determines possible reductions in the strengthened element capacity. This effect appears particularly critical in the case of cyclic and dynamic loads.
In this paper, the cyclic behavior of a PBO FRCM composite is experimentally investigated using low-cycle tensile tests on composite specimens. Namely, FRCM rectangular coupons are subjected to clamping- and clevis-grip tensile tests. These tests provide important information on the effect of low-frequency dynamic loading on the composite tensile properties under different test configurations.

Keywords: FRCM, TRM, PBO, Cyclic loading, Fatigue, Clevis-grip, Clamping-grip, Tensile behavior.

ISSN:2623-3347
Peer-review under responsibility of the organizing committee of COMPDYN 2023.
doi: 10.7712/120123.10560.21010

1 INTRODUCTION

In the last decade, fiber-reinforced cementitious matrix (FRCM) composites have been proposed as an alternative to fiber-reinforced polymer (FRP) composites in the strengthening of existing concrete [1] and masonry structures [2,3]. FRCM are comprised of high strength textiles embedded within an inorganic matrix and are applied onto the surface of existing members to increase their bending, shear, and torsional strength [4–6] and to provide confinement for axially-loaded members [7]. They have a high strength-to-weight ratio, physico-chemical compatibility with the substrate, and are easy to apply [8]. In recent years, FRCMs were proven to be an effective strengthening technique also for members subjected to cyclic loading [9,10]. Indeed, structures as bridges and viaducts are subjected to vehicular traffic that induces fatigue loads that may affect both the load-carrying capacity and durability of the structural element. Externally bonded (EB) FRCM were proposed as a possible strengthening solution, since they help to reduce the stress level in the existing member, thus extending its fatigue life. For instance, in EB FRCM RC beams subjected to fatigue loading, thinner and more spaced flexural cracks develop at the serviceability limit state in comparison with the corresponding unstrengthened RC beam [11,12].

Studies on FRCMs coupons demonstrated that they can resist to low-cycle fatigue tensile tests. Indeed, FRCM coupons showed a limited reduction of tensile properties in the post-fatigue quasi-static tensile test with respect to the corresponding quasi-static tensile tests. However, the presence of friction between the textile and embedding matrix represents an issue and a potential cause of fiber damage when the FRCM is subjected to cyclic loading [12].

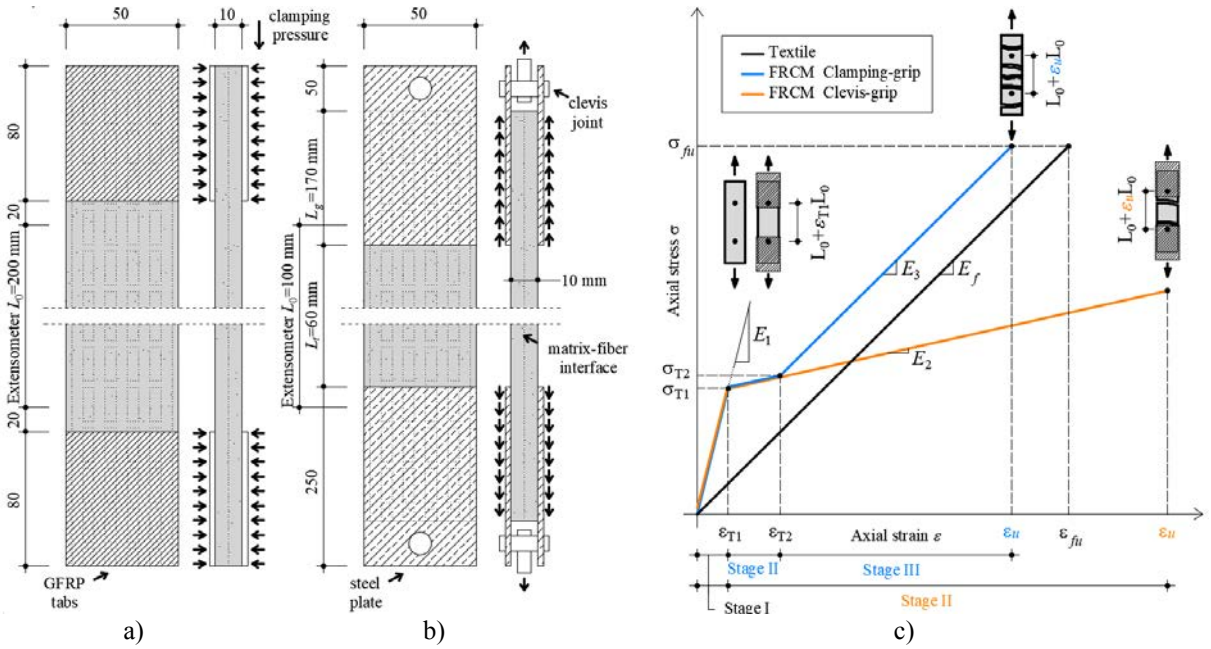

Figure 1: (a) Clamping- and (b) Clevis-grip tensile test set-ups and (c) corresponding stress responses.

Different test set-ups were proposed in the literature to study the FRCM composite tensile behavior [13]. Among them, the clamping- and clevis-grip test set-ups were adopted by the current Italian [14] and American [15] acceptance criteria for externally bonded inorganic-matrix composites, respectively. Figure 1a and b show a sketch of these set-ups. In clamping-grip tests (Figure 1a), the two ends of the specimen are clamped by the testing machine heads and then pulled apart while the textile slippage is hindered by the clamping pressure. The specimen failure generally occurs due to tensile rupture of the textile. In clevis-grip tests (Fig-

ure 1b), metallic plates are bonded to the lateral faces of the composite coupon and then connected to the testing machine with a clevis-type joint. Accordingly, the stress is transferred from the matrix to the textile mainly through shear (bond) stress. Failure typically occurs due to loss of bond (i.e., debonding) between fiber and matrix at the matrix-fiber interface [16].

Clamping- and clevis-grip test set-ups generally provide significantly different results due to the different boundary conditions of the specimen. The clamping-grip tensile test is employed to obtain information on the mechanical properties of the FRCM and of its component materials, whereas the clevis-grip tensile test allows for the investigation of the matrix-fiber stress transfer mechanism. The idealized axial stress σ - axial strain ε response of a FRCM clamping-grip test is trilinear, as shown in Figure 1c. The axial stress is conventionally computed as the ratio between the applied load and the textile cross-sectional area A_f. The first linear branch (Stage I in Figure 1c) is representative of the specimen uncracked stage and has a slope, E_1, associated with the matrix elastic modulus E_m ($E_1 A_f/A_m \approx E_m$, where A_m is the matrix cross-sectional area). Stage I ends when the tensile strength of matrix $\sigma_{m,u}$ ($\sigma_{T1} A_f/A_m \approx \sigma_{m,u}$) is reached, corresponding with a FRCM coupon strain value ε_{T1}. Further increases of the applied displacement result in the progressive occurrence of new matrix cracks (Stage II). This cracking process occurs at an approximatively constant or slightly ascending stress level, which determines a limited slope of the stress-strain curve, E_2. When no further matrix cracks occur, Stage II ends and the applied load is mainly carried by the reinforcing textile. During Stage III, the stress-strain curve slope is approximatively equal to the bare textile elastic modulus ($E_3 \approx E_f$). Specimen failure occurs when the tensile strength of fibers, σ_{fu}, is reached, or even at a lower stress level due to possible uneven distribution of stresses across the textile or textile damage induced by matrix-textile friction.

The idealized response of clevis-grip tensile tests is bilinear. Stage I of clevis-grip tensile tests is analogous to that of clamping-grip tests and ends when the matrix tensile strength is reached. Stage II of clevis-grip tests is characterized by the cracking of the matrix and (possible) relative displacement between textile and matrix due to the lack of clamping pressure at the specimen ends. The slope of the initial portion of Stage II of the clevis-grip response, E_2, can be similar to that observed in Stage II of clamping-grip tests. Failure generally occurs due to debonding at the matrix-fiber interface at a stress value lower than the textile tensile strength. However, failure of the textile may occur provided that the metallic plate-matrix bonded length is sufficient to allow for the development of bond stresses able to induce textile rupture [17]. Furthermore, rupture of sleeve textile filaments within fiber yarns or matrix splitting at the fiber-matrix interface may occur [18].

In this paper, the tensile behavior of a PBO FRCM is investigated using both clamping- and clevis-grip tensile tests. Namely, the effect of cyclic loading on the composite stress-strain response is analyzed. Fifteen load cycles with 1 Hz frequency were applied to the composite specimens, with the load ranging between 5% and 90% of the corresponding quasi-static characteristic tensile strength [19]. The influence of cyclic loading on the composite tensile strength, ultimate strain, and slopes of the stress-strain curve was investigated with reference to the specific behavior provided by each set-up considered.

2 MATERIALS AND METHODS

Eight PBO FRCM specimens were considered in this study. Four were tested using a clamping-grip set-up and the remaining four with a clevis-grip set-up. For each group, three specimens were employed for the quasi-static characterization of the composite tensile behavior, whereas one was subjected to cyclic loading. Specimens subjected to the clamping-grip test were named according to the notation T(or TF)_400_50_*n*, where T (=tensile) or TF

(=tensile cyclic) indicates the test type, 400 and 50 indicate the specimen length and width in mm, respectively, whereas *n* is the specimen number. Clevis-grip specimens were named TC(or TCF)_170_60_50_n, where TC (=tensile clevis) or TCF (=tensile clevis cyclic) indicates the test type, 170 and 60 indicate the clevis grip length L_g and the specimen free length L_t (see Figure 1) in mm, respectively, 50 is the specimen width in mm, and *n* is the specimen number. Quasi-static clevis specimens TC_170_60_50_1-3 were previously presented in [20].

2.1 Materials

The PBO FRCM composite investigated was comprised of one layer of textile [21] embedded within two 5 mm-thick layers of cement-based matrix [22]. The PBO textile had an unbalanced open-mesh geometry with longitudinal (i.e., aligned with the load direction) and transversal yarns having 70 and 18 g/m^2 area weight, respectively. Longitudinal yarns had a cross-sectional area of 0.46 mm^2 and were spaced at 10 mm on center. The tensile strength, ultimate strain, and elastic modulus of textile were previously measured by the authors [23] by testing 9 rectangular bare textile samples including 5 longitudinal yarns (according to [19]) and were equal to 3960 MPa (CoV=0.07), 1.65% (CoV=0.08) and 241 GPa (CoV=0.05), respectively. The compressive and flexural strength of the cement-based matrix were experimentally obtained by Bertolli and D'Antino [24] according to UNI EN 1015-11 [25] and were equal to 51.6 MPa (CoV=0.03) and 8.10 MPa (CoV=0.16), respectively.

2.2 Specimen geometry and test set-up

The FRCM rectangular coupons considered for this study were realized according to the indications of the European Assessment Document for inorganic-matrix composites [19]. Each specimen included 5 longitudinal yarns, which provided an overall textile cross-sectional area A_f=2.3 mm^2, and had nominal dimensions equal to 400 mm (length), 50 mm (width), and 10 mm (thickness).

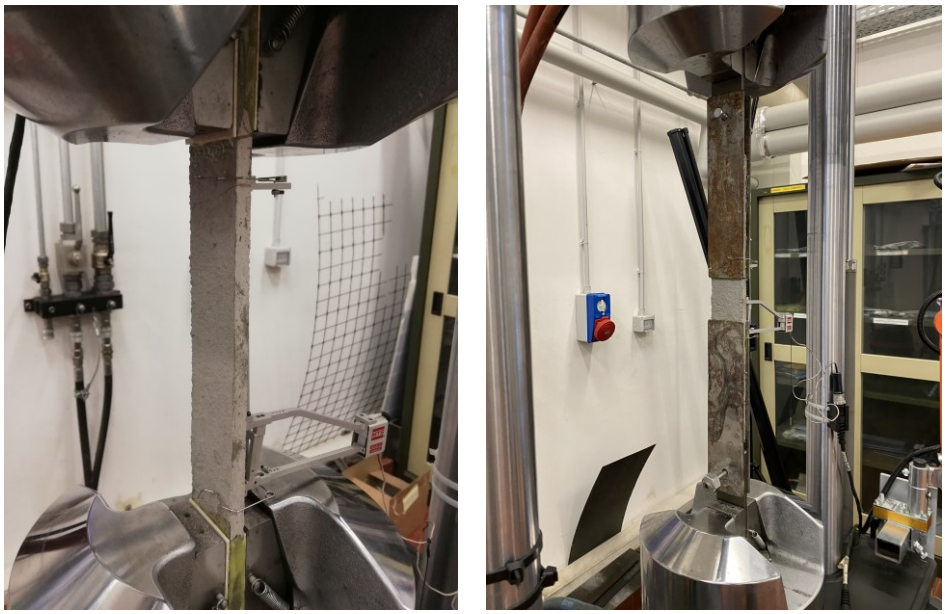

a) b)

Figure 2: Photos of tensile test set-ups: a) clamping-grip and b) clevis-grip.

Clamping-grip specimens were tested following the indications of [19]. Accordingly, the coupon ends were clamped by the testing machine gripping wedges applying enough pressure

to prevent, as much as possible, the textile slippage within the gripped length (see Figure 1a). In order to promote an even distribution of the clamping pressure, GFRP tabs of dimensions 80 mm (length) × 50 mm (width) × 2 mm (thickness) were epoxy-bonded to the coupon ends. An extensometer having a gauge length L_0=200 mm was applied to the specimen central portion to record the axial strain throughout the test (see Figure 2a). Clamping-grip quasi-static tests were conducted in displacement (stroke) control by monotonically increasing the machine head displacement at the rate of 0.2 mm/min. When the specimen entered its cracked stage (Stage III, see Figure 1c) the displacement rate was increased to 0.5 mm/min until the specimen failure.

Specimens tested with the clevis-grip configuration were equipped with 250 mm-long steel plates epoxy-bonded to the specimen ends and connected to the testing machine with spherical joints (see Figure 2b). The axial strain was recorded by an extensometer having gauge length L_0=100 mm, mounted to the central portion of the specimen with knives applied to the steel plates (see Figures 1b and 2b). Quasi-static tests were conducted following the indications of the American Acceptance criteria for inorganic matrix composites [15]. Accordingly, tests were conducted in stroke control at a constant rate of 0.2 mm/min.

2.3 Parameters of the cyclic tests

One specimen for each test configuration was subjected to a cyclic load with a 1 Hz frequency and with applied stresses ranging between $\sigma_{min}=0.05\sigma_{u,ck}$ and $\sigma_{max}=0.90\sigma_{u,ck}$, being $\sigma_{u,ck}$ the characteristic quasi-static tensile strength of the PBO FRCM composite. The characteristic values of the tensile strength declared by the composite manufacturer were $\sigma_{u,ck}$=2440 MPa for the clamping-grip set-up and $\sigma_{u,ck}$=1750 MPa for the clevis-grip set-up [21]. Specimens were initially subjected to the previously described quasi-static displacement-controlled mode until the attainment of the mean cyclic stress. The test control mode was then switched into force control and 15 load cycles were applied to the specimens according to a sinusoidal wave input. At the end of the cyclic stage, the load was maintained at a constant value equal to the mean cycle stress. Finally, a quasi-static test was performed in displacement control mode until the specimen failure.

3 RESULTS AND DISCUSSION

Table 1 reports the main parameters of the stress-strain response of the specimens considered in this study, along with averages and CoV of nominally equal quasi-static specimens.

Specimen	σ_{min} [MPa]	σ_{max} [MPa]	P_u [kN]	σ_u [MPa]	ε_u [%]	E_3 or E_2 [GPa]
T_400_50_1	-	-	7.05	3066	1.50	2005
T_400_50_2	-	-	7.43	3232	1.76	1728
T_400_50_3	-	-	6.75	2933	1.39	1974
Average (CoV%)	-	-	7.08(4.8)	3077(4.8)	1.55(12.3)	1902(8.0)
TF_400_50_1	130	2200	7.80	3389	1.97	1962
TC_170_60_50_1	-	-	4.35	1893	2.95	535
TC_170_60_50_2	-	-	3.91	1701	2.52	415
TC_170_60_50_3	-	-	4.21	1831	2.93	530
Average (CoV%)	-	-	4.16(5.4)	1808(5.4)	2.80(8.6)	493(13.8)
TCF_170_60_50_1	110	1580	4.95	2153	2.99	645

Table 1: stress-strain response parameters of the tested specimens.

The parameters studied include the maximum load recorded during the test (P_u), the specimen tensile strength ($\sigma_u=P_u/A_f$), the corresponding strain (ε_u), and the moduli E_3 and E_2 for the clamping-grip and clevis-grip specimens, respectively (see Figure 1c). In Table 1, E_3 and E_2 were computed as secant moduli between the stress-strain curve points associated with the stress values $0.6\sigma_u$ and $0.9\sigma_u$.

3.1 Quasi-static tests

Figure 3a and b show the stress-strain response of clamping- and clevis-grip specimens, respectively, where the axial stress $\sigma=P/A_f$ is the ratio between the applied load, P, and the fiber cross-sectional area, A_f, whereas the axial stain, ε, was measured by the extensometer.

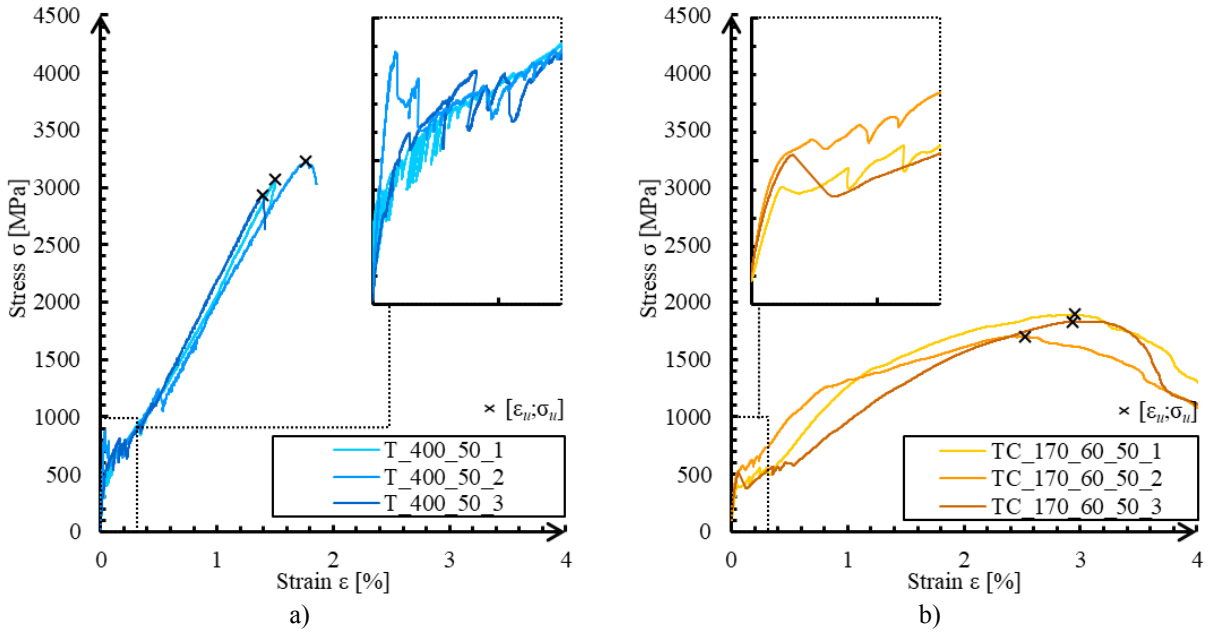

Figure 3: Stress-strain responses of quasi-static tests: a) clamping-grip and b) clevis-grip.

Specimens tested with the clamping-grip configuration (see Figure 3a) exhibited an approximately trilinear stress response, with an initial linear branch associated with the specimen uncracked stage. During the uncracked stage, the mechanical properties of the composite were mainly associated with those of the mortar matrix. Once the matrix tensile strength was reached, a first transversal crack opened and a marked stress drop was observed in the stress-strain curve. Beyond this point, several other cracks appeared in the matrix. The formation of new cracks corresponded with further stress drops in the specimen response and determined a gradual reduction of the stress-strain curve slope. When crack saturation was attained, the third linear branch of the σ-ε curve began, which was mainly governed by the tensile behavior of the textile. Specimen failure occurred due to fiber rupture at an applied stress σ_u corresponding to the axial strain ε_u (point [ε_u; σ_u] in Figure 3a). The tensile strength exhibited by the three clamping-grip specimens was slightly different due to possible unevenness in the applied load distribution among textile filaments, as commonly observed in FRCM composite tensile tests [26].

Figure 3b shows the stress responses of the three specimens tested with the clevis-grip configuration. The tensile response of specimens TC_170_60_50_1-3 was characterized by an initial linear branch associated with the specimen uncracked stage, which resembled that of clamping-grip specimens. The following cracked stage was characterized by the formation of

only two transversal cracks, which were located close to the edges of the specimen free portion due to stress concentrations caused by the presence of the steel plates [17]. During this second stage, the response became nonlinear due the slippage of textile within the embedding matrix, whereas the applied load increased due to the matrix-fiber stress transfer mechanism [24]. The maximum stress recorded during this stage was associated with point [ε_u;σ_u] (Figure 3b). After the attainment of the peak stress, the load response showed a decreasing branch. For all specimens, failure was characterized by a large opening of one of the matrix cracks and by significant textile slippage.

3.2 Cyclic tests

The stress-strain responses of specimens subjected to cyclic loading are presented in Figure 4, which includes the initial quasi-static loading stage, the 15 load-controlled cycles, and the post-cyclic quasi-static stage until failure. Envelopes of stress responses of corresponding quasi-static tests are also reported in Figure 4.

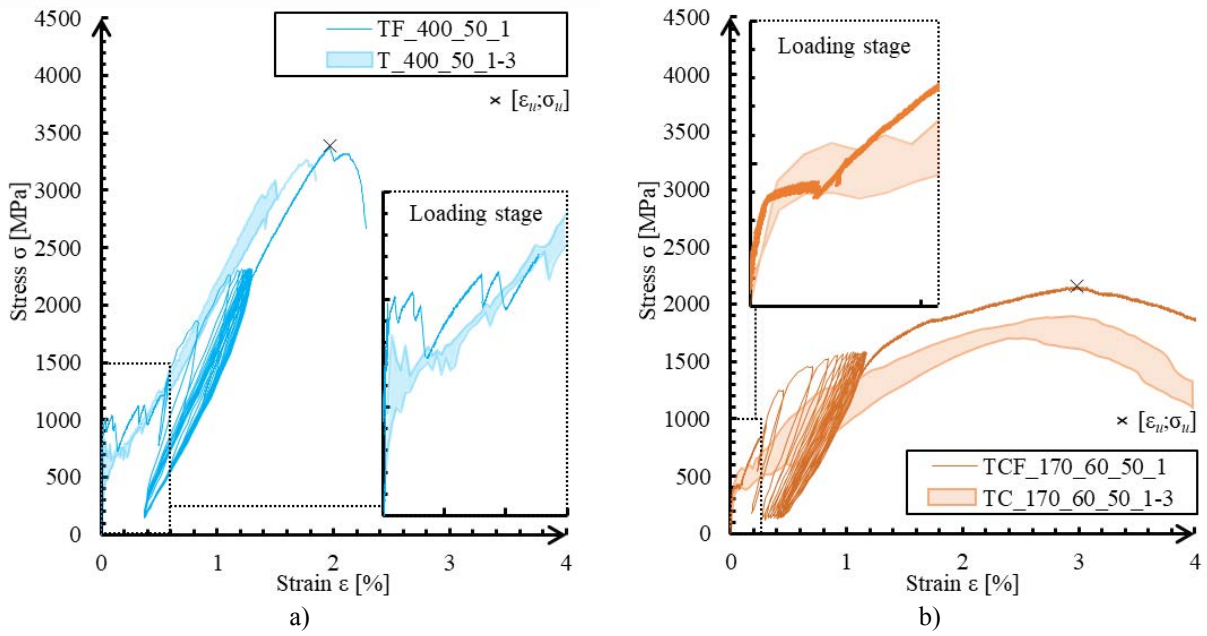

Figure 4: Stress-strain responses of cyclic tests: a) clamping-grip and b) clevis-grip.

As shown in Figure 4a, the first quasi-static load response of specimen TF_400_50_1 was consistent with that of corresponding quasi-static specimens. During this stage, several cracks formed in the matrix (as shown by the stress drops in the σ-ε curve) and crack saturation was attained before the mean cyclic stress was reached. Accordingly, the specimen stress response during load cycles was mainly governed by the textile tensile behavior. The cyclic stage of specimen TF_400_50_1 was characterized by a gradual reduction of the cycle secant modulus (i.e., the slope of the straight line connecting the peak and valley points of a load cycle). At the same time, a progressive increase of the axial strain at peak of each cycle was recorded, while the strain associated with the cycle valley point did not vary during the cyclic stage. This indicated that the specimen was able to fully recover its axial deformation at the end of each cycle, which could be attributed to absence of fiber slip within the clamped portions due to the presence of the clamping pressure. The post cyclic stress response resembled that of quasi-static specimens. The retained E_3 modulus and ultimate stress σ_u, i.e., the ratio between

the post-cyclic and average quasi-static values, were 103% and 110%, respectively, which indicated a limited influence of the cyclic load on the specimen tensile stiffness and strength.

The stress response of specimen TCF_170_60_50_1, tested with the clevis-grip set-up, is presented in Figure 4b. In this case, a gradual increase of the axial strain at peak and valley of each cycle was observed during the cyclic stage, while the secant modulus remained approximately constant. During the cyclic test, the peak stress σ_{max} was attained at a strain significantly lower than that associated with the same stress value of corresponding quasi-static tests (Figure 4b). The cyclic load determined a load response completely different from that observed with the quasi-static load, which can be attributed to the different load rate of the two tests. Indeed, PBO FRCM composites were reported to be rate dependent [27] and this peculiar behavior could be exploited when the composite is subjected to dynamic loads, as in the case of seismic actions. Further investigations are needed to study this behavior also for FRCM-strengthened members.

4 CONCLUSIONS

- Clamping- and clevis-grip test set-ups provided significantly different stress responses for the PBO FRCM investigated in this study due to their different boundary conditions. In the former case, a trilinear response was observed and failure occurred due to textile rupture. In the latter case, the behavior was bilinear and failure occurred with significant matrix-fiber slippage.
- The crack pattern exhibited by clamping- and clevis-grip tests was different. Several matrix cracks opened during Stage II of clamping-grip tests, whereas only two cracks, located close to the edges of the specimen free portion, were observed in clevis-grip tests.
- The cyclic load did not significantly affect the response of clamping-grip tests. This was attributed to the clamping pressure, which limited the textile slippage during the cyclic stage.
- The cyclic response of the specimen tested with the clevis-grip set-up was characterized by increasing values of strain associated with the peak and valley of each cycle. This indicated that the textile progressively slipped within the matrix during the cycles.
- The cycle peak stress σ_{max} of clevis-grip specimens was reached at a strain significantly lower than that associated with the same stress of corresponding quasi-static specimens. This behavior could be attributed to the rate effect observed in PBO FRCM composites.

REFERENCES

[1] Täljsten B, Blanksvärd T. Mineral-based bonding of carbon FRP to strengthen concrete structures. Journal of Composites for Construction 2007;11:120–8. https://doi.org/10.1061/(ASCE)1090-0268(2007)11:2(120).

[2] Papanicolaou CG, Triantafillou TC, Papathanasiou M, Karlos K. Textile reinforced mortar (TRM) versus FRP as strengthening material of URM walls: Out-of-plane cyclic loading. Materials and Structures/Materiaux et Constructions 2008;41:143–57. https://doi.org/10.1617/s11527-007-9226-0.

[3] de Felice G, De Santis S, Garmendia L, Ghiassi B, Larrinaga P, Lourenço PB, et al. Mortar-based systems for externally bonded strengthening of masonry. Mater Struct 2014;47:2021–37. https://doi.org/10.1617/s11527-014-0360-1.

[4] Bencardino F, Carloni C, Condello A, Focacci F, Napoli A, Realfonzo R. Flexural behaviour of RC members strengthened with FRCM: State-of-the-art and predictive formulas. Composites Part B: Engineering 2018;148:132–48. https://doi.org/10.1016/j.compositesb.2018.04.051.
[5] Loreto G, Babaeidarabad S, Leardini L, Nanni A. RC beams shear-strengthened with fabric-reinforced-cementitious-matrix (FRCM) composite. Int J Adv Struct Eng 2015;7:341–52. https://doi.org/10.1007/s40091-015-0102-9.
[6] Alabdulhady MY, Sneed LH. Torsional strengthening of reinforced concrete beams with externally bonded composites: A state of the art review. Construction and Building Materials 2019;205:148–63. https://doi.org/10.1016/j.conbuildmat.2019.01.163.
[7] Di Ludovico M, Prota A, Manfredi G. Structural Upgrade Using Basalt Fibers for Concrete Confinement. J Compos Constr 2010;14:541–52. https://doi.org/10.1061/(ASCE)CC.1943-5614.0000114.
[8] Koutas LN, Tetta Z, Bournas DA, Triantafillou TC. Strengthening of Concrete Structures with Textile Reinforced Mortars: State-of-the-Art Review. J Compos Constr 2019;23:03118001. https://doi.org/10.1061/(ASCE)CC.1943-5614.0000882.
[9] Calabrese AS, D'Antino T, Colombi P, Carloni C, Poggi C. Fatigue Behavior of PBO FRCM Composite Applied to Concrete Substrate. Materials 2020;13:2368. https://doi.org/10.3390/ma13102368.
[10] Calabrese AS, D'Antino T, Colombi P, Carloni C, Poggi C. Fatigue Behavior of FRCM Strengthened RC Beams: State of the Art and Future Developments. In: Ilki A, Ispir M, Inci P, editors. 10th International Conference on FRP Composites in Civil Engineering, vol. 198, Cham: Springer International Publishing; 2022, p. 201–12. https://doi.org/10.1007/978-3-030-88166-5_16.
[11] Leung CKY, Cheung YN, Zhang J. Fatigue enhancement of concrete beam with ECC layer. Cement and Concrete Research 2007;37:743–50. https://doi.org/10.1016/j.cemconres.2007.01.015.
[12] Calabrese AS, D'Antino T, Colombi P, Poggi C. Low- and High-Cycle Fatigue Behavior of FRCM Composites. Materials 2021;14:5412. https://doi.org/10.3390/ma14185412.
[13] D'Antino T, Papanicolaou C (Corina). Comparison between different tensile test setups for the mechanical characterization of inorganic-matrix composites. Construction and Building Materials 2018;171:140–51. https://doi.org/10.1016/j.conbuildmat.2018.03.041.
[14] CSLLPP. Linee guida per la identificazione, la qualificazione ed il controllo di accettazione di compositi fibrorinforzati a matrice inorganica (FRCM) da utilizzarsi per il consolidamento strutturale di costruzioni esistenti. Rome, Italy: 2022.
[15] International Code Council Evaluation Service (ICC-ES). Acceptance criteria for masonry and concrete strengthening using fabric-reinforced cementitious matrix (FRCM) and steel reinforced grout (SRG) composite systems. AC434. Whittier, CA: 2018.
[16] Donnini J, Chiappini G, Lancioni G, Corinaldesi V. Tensile behaviour of glass FRCM systems with fabrics' overlap: Experimental results and numerical modeling. Comp Struct 2019;212:398–411. https://doi.org/10.1016/j.compstruct.2019.01.053.
[17] Focacci F, D'Antino T, Carloni C. Tensile Testing of FRCM Coupons for Material Characterization: Discussion of Critical Aspects. Journal of Composites for Construction 2022;26:04022039. https://doi.org/10.1061/(ASCE)CC.1943-5614.0001223.
[18] Campanini D, Hadad HA, Carloni C, Mazzotti C, Nanni A. Mechanical Characterization of SRG Composites According to AC434. Key Engineering Materials 2019;817:458–65. https://doi.org/10.4028/www.scientific.net/KEM.817.458.

[19] EOTA. EAD 340275-00-0104: Externally-bonded composite systems with inorganic matrix for strengthening of concrete and masonry structures 2018.
[20] D'Antino T, Calabrese AS, Colombi P, Poggi C. Experimental and numerical investigation on the tensile behavior of PBO FRCM composites with textile lap splice. Construction and Building Materials 2023;363. https://doi.org/10.1016/j.conbuildmat.2022.129437.
[21] Ruregold. Technical datasheet of PBO-MESH 70/18 2022.
[22] Ruregold. Technical datasheet of MX-PBO CALCESTRUZZO 2019.
[23] Calabrese AS, D'antino T, Colombi P, Poggi C. Long-Term Behavior of PBO FRCM and Comparison with Other Inorganic-Matrix Composites. Materials 2022;15. https://doi.org/10.3390/ma15093281.
[24] Bertolli V, D'Antino T. Modeling the behavior of externally bonded reinforcement using a rigid-trilinear cohesive material law. International Journal of Solids and Structures 2022;248:111641. https://doi.org/10.1016/j.ijsolstr.2022.111641.
[25] UNI EN 1015-11, Metodi di prova per malte per opere murarie – Determinazione della resistenza a flessione e a compressione della malta indurita n.d.
[26] Caggegi C, Lanoye E, Djama K, Bassil A, Gabor A. Tensile behaviour of a basalt TRM strengthening system: Influence of mortar and reinforcing textile ratios. Composites Part B: Engineering 2017;130:90–102. https://doi.org/10.1016/j.compositesb.2017.07.027.
[27] Carloni C, Verre S, Sneed LH, Ombres L. Loading rate effect on the debonding phenomenon in fiber reinforced cementitious matrix-concrete joints. Compos Part B 2017;108:301–14. https://doi.org/10.1016/j.compositesb.2016.09.087.